RSC Advances

PAPER

View Article Online
View Journal | View Issue

Open Access Article. Published on 23 June 2017. Downloaded on 10/24/2025 10:46:36 PM.
This article is licensed under a Creative Commons Attribution-NonCommercial 3.0 Unported Licence.

Check for updates

Cite this: RSC Adv., 2017, 7, 32236

In situ inorganic flame retardant modified hemp and its polypropylene composites

W. J. Zhao,[a] Q. X. Hu,[a] N. N. Zhang,[a] Y. C. Wei,[a] Q. Zhao,[a] Y. M. Zhang,[a] J. B. Dong,[a] Z. Y. Sun,[b] B. J. Liu,[c] L. Li[d] and W. Hu *[a]

Received 10th April 2017
Accepted 13th June 2017

DOI: 10.1039/c7ra04078d

rsc.li/rsc-advances

A hemp-reinforced polypropylene (PP) composite with excellent flame retarding and mechanical properties was prepared with the melt blending method. Hemp fiber (F) was first simply *in situ* modified with an inorganic salt solution, which was prepared by mixing 4.32% sodium hydrate (NaOH) and 6% calcium chloride ($CaCl_2$) at room temperature for 0.5 h. The modified hemp (F1) was proved to be modified by the calcium salt through Fourier-transform infrared and scanning electron microscopy (SEM) measurements. The thermal stability, mechanical, and flame retarding properties of the composites were studied by thermogravimetric analysis, mechanical tests, and limiting oxygen index (LOI) measurements, respectively. The LOI of the composites with 50% of F1 and 15% poly(phosphoric acid amine) reached 25.5%, which was much higher than that of PP (18.5%). The tensile strength of the composite with 50% of F1 was 38% higher than that of PP (24 MPa). The composite interface between the F1 and PP matrix was investigated by SEM, and was shown to be significantly improved. This showed that *in situ* inorganic modification of hemp with a mixture of NaOH and $CaCl_2$ is a promising method to improve both the flame retarding and mechanical properties of the biocomposite.

Introduction

Biocomposites reinforced with natural fibers have been an attractive research subject worldwide. Fibers, such as jute, ramie, sisal, flax and hemp can be obtained from natural resources.[1,2] Natural-fiber-based biocomposites present several advantages, such as good mechanical properties, biodegradability, low cost, low density, low energy consumption, and environmental friendliness,[3–7] and they have been widely applied in many fields, such as automotive, marine, building, transportation, and so on.[1,8] However, natural fibers are very flammable and hydrophilic, which also results in flammability and worse interfacial properties of their reinforced biocomposites, and restricts their application. Therefore, modifications of natural fibers are necessary to improve their fire resistance and hydrophobicity.[1,9,10] As a type of widely applied natural fiber, hemp also presents hydrophilicity and poor fire resistance.

Flammability is one of the important properties of natural fiber/polymer composites.[11] The flame-retardant properties of composites can be improved by adding a flame retardant into the composites.[12] Reports were found on the application of intumescent ammonium polyphosphate (APP) on kenaf natural fiber/polypropylene (PP) composite.[13,14] Inorganic hydroxides, such as $Mg(OH)_2$ and $Al(OH)_3$, could also be applied as flame retardant for composites.[15] $Mg(OH)_2$ was applied to improve the flammability of the sisal/PP composite.[6] It was also directly incorporated into sawdust/PP composites. Consequently, the burning rate of the composite with 25% $Mg(OH)_2$ decreased by 34.7% compared with that of pure PP.[16] However, the mechanical properties of the composites decreased when the flame retardants were added.

On the other hand, the hydrophilic surface of the natural fiber results in its bad interfacial property with the hydrophobic matrix, such as polyolefin. The bad interface leads to the decreased mechanical properties of the composites.[10,17] Chemical modification and coupling agents are effective methods to transform natural fiber from hydrophilic into hydrophobic.[17,18] Moreover, alkali treatment is always applied first to remove the impurities, lignin, and hemicellulose on the fiber surface, which exposes more hydroxyl groups for further modification. Also, alkali could react with the hydroxyl group, and thereafter negative oxygen ion can be produced.[19] Among the coupling agents, maleic-grafted polypropylene (MAPP) is very efficient in improving the interfacial property of natural fiber-reinforced composites with approximately 2% added in the system.[20]

So far, few reports exist about another cheap alkaline-earth metal hydroxide, calcium hydroxide ($Ca(OH)_2$), which could

[a]College of Chemical Engineering, Changchun University of Technology, 2055 Yan'an Street, Changchun 130012, P. R. China. E-mail: huwei@ccut.edu.cn; Fax: +86-431-85717216; Tel: +86-431-85717216

[b]State Key Laboratory of Polymer Physics and Chemistry, Changchun Institute of Applied Chemistry, Chinese Academy of Sciences, Changchun 130022, China

[c]College of Chemistry, Jilin University, 2699 Qianjin Street, Changchun 130012, P. R. China

[d]School of Life Science and Technology, Harbin Institute of Technology, Harbin, 150080, P. R. China

This journal is © The Royal Society of Chemistry 2017

Open Access Article. Published on 23 June 2017. Downloaded on 10/24/2025 10:46:36 PM.
This article is licensed under a Creative Commons Attribution-NonCommercial 3.0 Unported Licence.

also function as a flame retardant. When $Ca(OH)_2$ is heated, it is decomposed into calcium oxide (CaO) and water. The water and CaO can help to stop the flame during firing.[21] This reaction and mechanism are similar to those related to $Mg(OH)_2$ and $Al(OH)_3$.[22,23] As the inorganic fire retardant material, $Mg(OH)_2$ and $Al(OH)_3$ are relatively not cheap because usually at least 25% of them are necessary to be applied for the satisfied fire retardant effect for the composites. In addition, the composite mechanical properties are always affected obviously after their insertion.

Given that the direct insertion of flame retardant into composites usually decreases the composite mechanical properties, in this work, the hemp was modified with the freshly prepared $Ca(OH)_2$ emulsion. The preparation method of $Ca(OH)_2$ emulsion was to mix the molar-equivalent alkali (NaOH) and calcium chloride ($CaCl_2$) solution. The modified hemp and its composites were characterized, and the synergistic effect of the inorganic modification with the coupling agent MAPP and the flame retardant APP was also examined. The study afforded a new promising modification method on hemp to improve both flame retarding and mechanical properties of the biocomposites.

Experimental

Materials

Hemp was received from Youma Company of Shandong Province, China. NaOH (98%), $CaCl_2$ (98%) was obtained from Tianjin Zhiyuan Chemical Reagent Co., Ltd. Polypropylene (PP1274) was received from Yang Rong Plastic raw material Co., Ltd of Guangdong Province, China. MAPP 7452 was received from Clariant, Germany. APP was received from Shandong Shian chemical Co., Ltd.

Hemp was cut into 3 mm of length. The obtained short fibers were washed with distilled water, and then were dried at room temperature for 8 h, and further oven dried at 120 °C for another 3 h. The fully dried fibers were stored in sealed plastic bag.

In situ inorganic treatment of hemp fiber

Mixing 4.32% NaOH (2.16 g, 0.054 mol) solution of 50 ml with 6% $CaCl_2$ (3 g, 0.027 mol) solution of 50 ml, respectively, to get a 2% $Ca(OH)_2$ (2 g, 0.027 mol) emulsion of 100 ml, in the light that 2 mol NaOH reacts with 1 mol $CaCl_2$ to get 1 mol $Ca(OH)_2$. The short hemp fiber of 10 g were immersed and soaked into 100 ml of such emulsion at room temperature as soon as possible, and then kept for 0.5 h with stirring. Thereafter, the treated fiber was washed with distilled water twice to remove the attached $Ca(OH)_2$, and dried at room temperature for 8 h, and further oven dried at 120 °C for 3 h to remove all the moisture in the fiber.

Preparation of thermal degraded hemp residue

The thermal degradation residue of the untreated and treated hemp fibers was prepared with a CQ-GS 10A pipe furnace from Luoyang Chunqing Furnace Industry Co., Ltd (Luoyang, China). The samples of F and F1 were initially heated from 50 °C to 300 °C or 500 °C with a heating rate of 10 °C min^{-1} and kept at 300 °C or 500 °C for 1 h. N_2 was flowed during the measurement. The thermal degradation residue of the untreated and treated hemp fibers treated at 300 °C were denoted as 300F and 300F1, respectively, and 500F and 500F1, respectively, for the materials treated at 500 °C. The chemical structure, surface morphology and crystallization were analyzed with FTIR, SEM and XRD measurement.

Preparation of hemp/PP composites

The hemp fiber, PP, APP and MAPP were oven dried at 80 °C for 12 h. They were mixed together in a plastic bag, and the bag was sealed tightly. The materials were then compounded using HAAKE mixer (PolyLab OS RheoDrive 7) with a speed of 60 rpm at 185 °C for 10 min. The formulation of the composites was listed in Table 1. The panel of composites was prepared by hot press at 185 °C for 3 min. The specimens for the mechanical test were taken from the panel.

Characterization

FTIR characterization. FTIR characterization of the untreated and treated fibers was performed with a Nicolet AVATAR-360 (USA) FTIR spectrometer by compressing samples on the stage in Attenuated Total Reflectance (ATR) transmittance mode in the wavenumber range of 4000–650 cm^{-1}. The frequency was 32 and the scan number was 256.

Fire resistance measurement. The oxygen index of the hemp fiber was measured according to the standard GB/T 5454-1997. LOI of the composites was obtained based on the standard ASTM D2863. The size of the specimens used for the flame retardant test was 100 mm × 6.5 mm × 3 mm. A Qingdao ShanFang M606B oxygen index apparatus was applied for the measurement. UL-94 vertical burning level was tested on a CZF-2 instrument (Jiangning, China) according to ASTM D 3801. The dimension of samples was 130 mm × 13 mm × 3.2 mm.

Table 1 Formulation of the composites[a]

Samples	PP (g)	F1 (g)	F (g)	MAPP (g)	APP (g)
PP	100	—	—	—	—
PPF-20	78	—	20	2	—
PPF1-20	78	20	—	2	—
PPF1-20-15R	63	20	—	2	15
PPF-30	68	—	30	2	—
PPF1-30	68	30	—	2	—
PPF1-30-10R	58	30	—	2	10
PPF1-30-15R	53	30	—	2	15
PPF1-30-20R	48	30	—	2	20
PPF-50	48	—	50	2	—
PPF1-50	48	50	—	2	—
PPF1-50-10R	38	50	—	2	10
PPF1-50-15R	33	50	—	2	15
PPF1-50-20R	28	50	—	2	20

[a] And at least five notched specimens were tested to obtain the average values.

Open Access Article. Published on 23 June 2017. Downloaded on 10/24/2025 10:46:36 PM.
This article is licensed under a Creative Commons Attribution-NonCommercial 3.0 Unported Licence.

Mechanical properties. The tensile strength and modulus of the PP and composites were measured according to ASTM D638 standard with a 3365 Instron universal tensile testing machine. Specimens were prepared according to the same standard. Crosshead speed was set as 1 mm min^{-1}. At least five specimens were tested to obtain the average values.

According to the GB 1451-83 standard, the impact testing was carried out with a XJU-22 test machine from Chengde material testing machine manufacturing plant, china. Specimens were prepared according to the same standard.

Interface morphology characterization. Scanning electron microscopy (JSM5600) was used to determine the morphology of F and F1, their thermal degradation residue, and the fractured surface of PP composites after broken in the liquid nitrogen. The specimens were coated with gold, which rendered them conductive to be scanned under the electron beam.

Thermal stability. Perkins-Elmer TGA thermal gravimetric analyzer was applied to characterize the thermal property of PP and hemp/PP composites with a heating rate of 20 °C min^{-1} from 25 °C to 600 °C. N_2 was flowed during the measurement.

Crystallization behaviour. Crystallization properties of the PP and composites were analyzed applying DSC1 Star System from Mettler Toledo Instruments, Swiss. The samples were initially heated from 25 to 210 °C with a heating rate of 20 °C min^{-1}, then cooled down to 25 °C with a cooling rate of 10 °C min^{-1}, finally reheated to 210 °C with a heating rate of 10 °C min^{-1}. N_2 was flowed during the whole measurement.

The degree of crystallizations was determined as follows:

$$X_c = (\Delta H_m/(w \times \Delta H_m^0)) \times 100\%$$

where ΔH_m is the experimental melting enthalpy (J g^{-1}) and ΔH_m^0 is the melting enthalpy of a pure crystalline matrix, PP (209 J g^{-1}).[24] w is the mass fraction of PP in the composite.

The crystallization behavior of PP, PP composites, and the thermal degradation residue 500F and 500F1 was measured with X-ray diffractometer D8 ADVANCE from BRUKER company (Germany). The samples were scanned in the angle range from 5° to 60°. The scanning speed was 2° min^{-1}.

Results and discussion

Modification effect on hemp

Fourier-transform infrared characterization. Fig. 1 shows Fourier-transform infrared (FTIR) spectra of hemp fiber (F) and the treated fiber (F1). And Fig. 1(b) is the magnification figure of 800–2000 cm^{-1} region in the FTIR spectra to show more clearly the absorption peaks in this region. The peak at 1425 cm^{-1} was ascribed to the symmetric CH_2 bending vibration attributed to the crystalline cellulose. The peak at 1725 cm^{-1} was the characteristic C=O peak stretching of carbonyl related to hemicellulose and lignin. While the peak at 1235 cm^{-1} was the characteristic peak of C–O stretching of the aryl group in lignin.[25] These peaks indicated that lignin and hemicelluloses existed in the untreated fiber specimens.

On the FTIR spectra of F1, the reduction of the peak at 1725 and 1235 cm^{-1} was observed and was attributed to the partial removal of lignin and hemicelluloses after modification. The removal of hemicellulose and lignin by alkali treatment caused the fibrils to rearrange themselves in a more compact manner and resulted in closer fiber packing, and thus the crystallinity of the fibers was also increased. This treatment thus could improve the fiber strength properties. In addition, the characteristic peak of the hydroxyl group improved after modification, as shown in Fig. 1. This improvement was due to the more hydroxyl groups exposed on the fiber surface after modification.[26,27] Our treatment effect was similar with that of NaOH treatment from the FTIR result, which proved that an extra NaOH existed in the system, or the fresh $Ca(OH)_2$ could also have the similar treatment effect on hemp as NaOH. Furthermore, the peak at 1411 cm^{-1} on the spectra of treated hemp fiber increased, and the small peak at 873 cm^{-1} appeared for the FTIR spectra of F1. This proved the formation of calcium carbonate during treatment.[28,29]

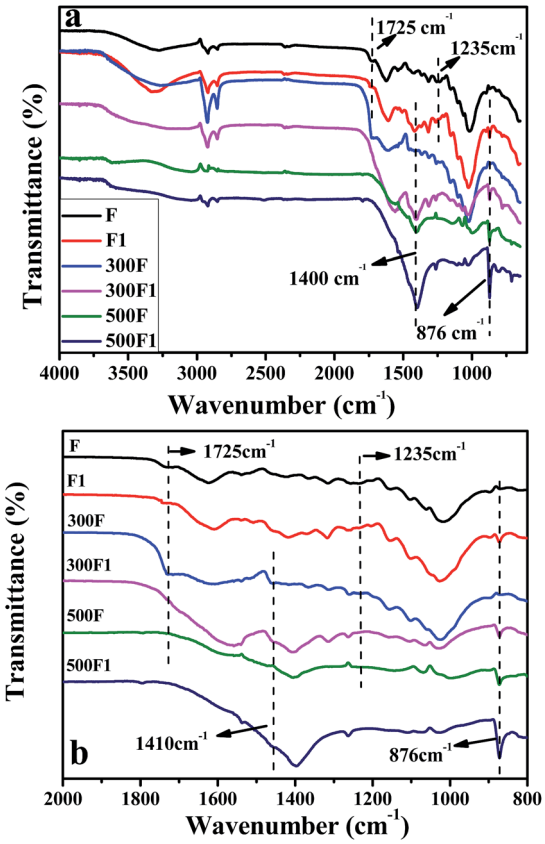

Fig. 1 FTIR spectra of the untreated hemp fiber F and treated hemp fiber F1, the thermal degradation residue 300F, 300F1, 500F and 500F1 (a); the enlarged spectra range of 750–2500 cm^{-1} (b).

When sodium hydroxide and calcium chloride were mixed together, calcium hydroxide ($Ca(OH)_2$) was immediately produced. The amount of NaOH and $CaCl_2$ added to the weight equivalent in the system was designed to induce a reaction.

The obtained $Ca(OH)_2$ could be slightly dissolved in the water. The hydroxyl group can react with NaOH, and a negative oxygen ion ($-O^-$) could be produced on the fiber surface. The free OH^- from the dissolved $Ca(OH)_2$ transferred into NaOH

Open Access Article. Published on 23 June 2017. Downloaded on 10/24/2025 10:46:36 PM.
This article is licensed under a Creative Commons Attribution-NonCommercial 3.0 Unported Licence.

with Na^+, and the produced NaOH reacted with the hydroxyl group on the hemp fiber into $-O^-Na^+$. However, the dissolved $Ca(OH)_2$ may react with the hydroxyl group on the fiber and the O^- was also produced.[18,19] Thus, calcium alkoxide was formed and grafted on the fiber surface. To obtain the potential balance, $-O^-Ca^{2+}-OH$ was formed. Thus, $-O^-Na^+$ and $-O^-Ca^{2+}-OH$ were produced on the fiber surface. The reaction scheme is shown in Scheme 1. During this process, the produced $Ca(OH)_2$ was continuously consumed, and the dynamic equilibrium caused it to continue dissolving. The undissolved $Ca(OH)_2$ was deposited on the fiber surface through hydrogen bond between the hydroxyl group and oxygen. Further, it could react with the CO_2 in the air into calcium carbonate.

Morphology observation. Fig. 2 shows the morphology photographs of F and F1, as obtained *via* scanning electron microscopy (SEM). Thick layers of cuticle (composed of lignin and hemicellulose) on the hemp surface were observed, as shown in Fig. 2(a). Fig. 2(b) shows that the fiber surface was coated with a layer of wax-like materials, and solid particles were inconsistently dispersed on the surface. These granules should be the $Ca(OH)_2$ and $CaCO_3$ produced after modification, which could not be fully washed off by the cleaning process.

Flammability of hemp fiber. Inorganic hydroxide $Mg(OH)_2$ and $Al(OH)_3$ are applied as flame retardant for natural fiber composites. As one of the alkaline-earth metal hydroxides, $Ca(OH)_2$ has seldom been applied as a fire retarder. In this study, $Ca(OH)_2$ was freshly *in situ* prepared and applied to modify hemp.

The limiting oxygen index (LOI) of the treated and untreated hemp fiber is shown in Table 2. The LOI tests characterize the minimum oxygen concentration required to support combustion. The LOI of the treated fiber was 25.5, which was obviously higher than that of the untreated fiber (20.5). This proved that our modification with the alkali and calcium chloride on the hemp can effectively improve the fire resistance of hemp. As shown in Scheme 1, after the modification, part of the produced calcium hydroxide $-O^-Ca^{2+}-OH$ and calcium carbonate $CaCO_3$ were deposited on the hemp fiber surface. During burning, $-O^-Ca^{2+}-OH$ reacted with CO_2, and $CaCO_3$ was also produced. When $CaCO_3$ was burned, calcium oxide CaO was created.[21,30–32] The CaO produced was attached to the combustible surface, which can further prevent the combustion from spreading. CaO can also continue to absorb the gas and smoke produced from the incomplete combustion of the polymer. It can absorb the half-burnt molten residue. Thus, the combustion of the treated hemp stopped immediately, thereby eliminating the smoke and preventing droplets, and the LOI was significantly increased.

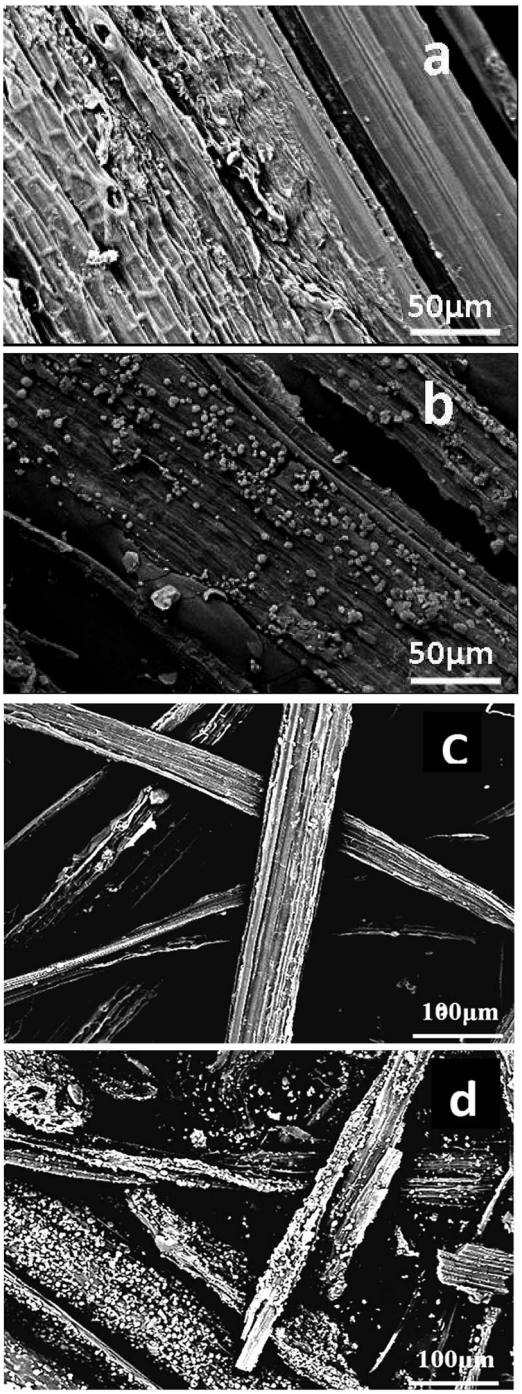

Fig. 2 SEM photos of the hemp fiber surface: (a) F; (b) F1, and the thermal degradation residue of hemp fiber surface: (c) 500F, (d) 500F1.

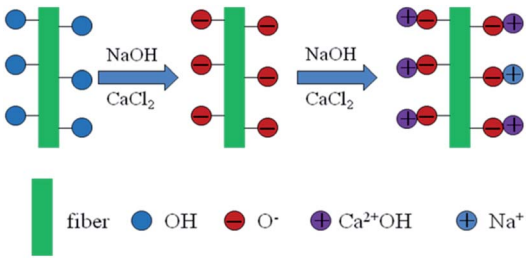

Scheme 1 Mechanism of the chemical treatment on the hemp.

Thermal degradation residue of hemp. Fig. 1 shows the FTIR spectra of the thermal degradation residue of F and F1 heated at 300 °C and 500 °C, respectively. Cellulose degrades at 300 °C.[33,34] The characteristic peak of –OH at 3000 cm^{-1} to 3700 cm^{-1} weakened with the heating temperature, which proved that the hydroxyl group of calcium hydroxide, $-O^-Ca^{2+}-OH$, and cellulose of hemp decreased with heating. The characteristic

Open Access Article. Published on 23 June 2017. Downloaded on 10/24/2025 10:46:36 PM.
This article is licensed under a Creative Commons Attribution-NonCommercial 3.0 Unported Licence.

Table 2 Limiting oxygen index of the treated and untreated hemp and their reinforced composites

Samples	Limiting oxygen index	UL-94
Untreated hemp	20.5	—
Treated hemp	25.5	—
PP	18.5	—
PP-15R	20.5	—
PPF-20	19.3	—
PPF-20-15R	21.2	—
PPF1-20	20.0	—
PPF1-20-15R	22.3	—
PPF-30	20.5	—
PPF-30-15R	22.3	—
PPF1-30	21.5	—
PPF1-30-10R	22.8	—
PPF1-30-15R	23.5	—
PPF1-30-20R	24.0	—
PPF-50	22.3	—
PPF-50-15R	24.3	0
PPF1-50	23.5	—
PPF1-50-10R	24.6	0
PPF1-50-15R	25.5	0
PPF1-50-20R	26.1	0

peaks of $CaCO_3$ were observed at 1400 cm^{-1} and 873 cm^{-1} for 300F1 compared with that of 300F.[29] The intensity of these peaks became more intensive compared with those of F1, as shown in Fig. 1. All attached $Ca(OH)_2$ should react with CO_2 during heating at 300 °C to produce $CaCO_3$. Furthermore, the calcium alkoxide produced after modification also reacted with CO_2 to produce $CaCO_3$. These peaks appeared on the FTIR spectra of 500F and 500F1 with even higher intensity. The calcium salt component found in hemp may react with CO_2 at 500 °C to produce $CaCO_3$. The more $CaCO_3$, the better flammability biocomposites present.

Fig. 3 shows the X-ray diffraction (XRD) patterns of thermal degradation residue of hemp produced at 500 °C. The magnification figure in the region 30 < 2 theta < 50 degrees are inserted as Fig. 3(b) to better understand the data. The diffraction peaks of 500F and 500F1 were at 23.05°, 29.4°, 36.12°, 39.4°, 43.12°, 47.12° and 48.54°. These are characteristic diffraction peaks of $CaCO_3$.[21,29] The peak intensity of 500F1 spectra was higher than that of 500F. This is consistent with the result of FTIR characterization. The calcium salt in F1 was further proven to exist.

Fig. 2(c) and (d) show the SEM photos of the thermal degradation residue of F and F1, respectively, which also showed the existence of some white granules on the surface of F1 compared with that of F even at 500 °C. The amount of white granules was much more than that on F1 as shown in Fig. 2(b). These white granules were determined to be $CaCO_3$ through FTIR and XRD characterization, and proved the calcium alkoxide also transferred into $CaCO_3$ during heating. When hemp was set on fire, thermal decomposition of $CaCO_3$ occurred, thereby absorbing the heat on the burning surface and producing CO_2 to stop the burning. Thus, hemp became

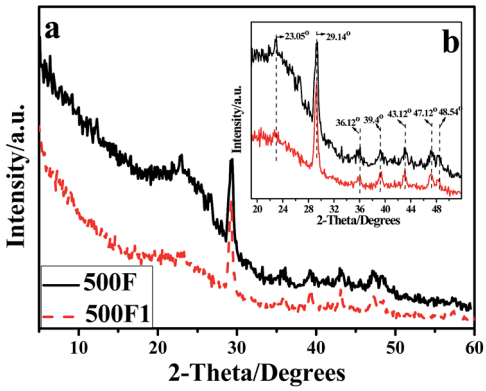

Fig. 3 WAXD curves of the 500F and 500F1 (a); the enlarged specta of the region 30 < 2-theta < 50 degrees (b).

a flame retardant after modification with *in situ* prepared calcium hydroxide.

Performance of hemp/PP composites

Flammability of PP composites. Table 2 and Fig. 4 shows the LOI value of PP and hemp/PP composites. The measurement result of UL-94 of the composites is also shown in Table 2. The LOI value of the composites was shown to be increased with the fiber ratio in the composites. The LOI of PPF-50 composite was 22.3, which was much higher than that of pure PP (LOI = 18.5). The reason should be that the hemp can behave as a type of char-forming agent, which can stop the burning from spreading and block oxygen. In addition, the LOI value of the modified hemp/PP composite was higher than that of the untreated hemp-reinforced composites. As an example, the LOI of PPF1-50 composite was 23.5. The fire resistance of our modified hemp reinforced PP composites could also be effectively improved, although PP is very flammable. To further improve the fire resistance of the composite, additional fire retardant, APP, was added to the composites. The LOI value of the composite with 20% hemp and 15% APP PPF-20-15R was 21.2, which was higher than that of PPF-20(19.3). And the LOI value of the composite increased with the APP content according to the comparison between the PP composite with 30% and 50% modified hemp

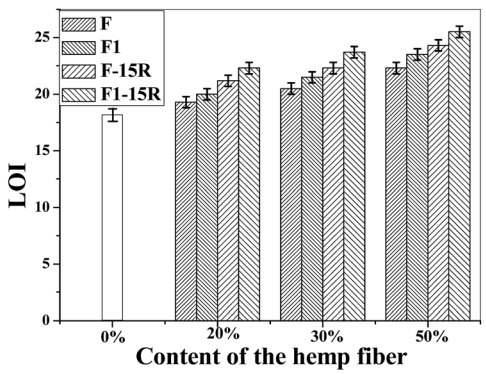

Fig. 4 Limiting oxygen index of the treated and untreated hemp and their reinforced composites.

Open Access Article. Published on 23 June 2017. Downloaded on 10/24/2025 10:46:36 PM.
This article is licensed under a Creative Commons Attribution-NonCommercial 3.0 Unported Licence.

and different APP content, as shown in Table 2. The LOI value of the PP composite with 50% modified hemp and 15% APP PPF1-50-15R increased to 25.5. And the UL-94 measurement result of PPF-50-15R, PPF1-50-10R, PPF1-50-15R and PPF1-50-20R was 0. This means theses composites can self-extinguish when they are fired.

As an intumescent flame retardant, APP helped to introduce more residual char, and thus improve the fire retardancy of the composite. When the composites with APP were heated and began to decompose, ammonia and a very stable poly(-phosphoric acid) were produced, and an insulating protective layer was formed on the material surface to block the oxygen for further burning. Therefore, the flammability resistance of composite was improved after adding APP.[11,12,14,35]

The LOI value of PPF1-50-10R was 24.6, and it could also self-extinguish according to the UL-94 test result, which means 10% APP was good enough for the composite fire resistance when modified fiber was 50%. For the better fire retardancy and low expenses of composites, PPF1-50-15R was applied for the further composite property study.

Mechanical properties. Many reports about the application of APP and inorganic hydroxides, such as $Mg(OH)_2$ and $Al(OH)_3$, on the flame retardant composites could be found.[6,13–15] The addition of a large amount of flame retardants to the composites could effectively improve the flammability of the composites. However, the mechanical properties of the composites were normally affected.

Fig. 5 shows the tensile strength (a) and modulus (b) of virgin PP and PP composites. Hemp fiber loading ratio in the composite was 0%, 20%, 30%, and 50%. The composite tensile strength and modulus increased with fiber loading ratio. When the hydrophilic hemp fiber was used to reinforce the hydrophobic polymer matrix, the poor compatibility between the natural fiber and polymer matrix usually result in bad mechanical properties. MAPP was reported to be a good compatibilizer for natural fiber/polymer composites. The mechanism is supposed to be the esterification between the anhydride groups of MAPP and the hydroxyl groups of the natural fiber.[18,20] In this work, MAPP was applied in all the composite formulations for the best mechanical property. With MAPP, the tensile strength of composite with 20% of untreated hemp fiber-reinforced PP composite (PPF-20) was 22.6 MPa, which was comparable with that of PP. Furthermore, the strength of the inorganic-modified hemp-reinforced composite PPF1-20 was 26.5 MPa. Both strength and modulus of PPF1-20 were much better than those of PPF-20. And similarly, PPF1-30 and PPF1-50 also presented better tensile properties than those of PPF-20 and PPF-20, respectively. The tensile strength of the composite reinforced with 50% treated hemp fiber PPF1-50 increased to 38% compared with that of pure PP, while its modulus was three times that of PP.

The result proved that our inorganic modification on hemp fibers could help to improve the tensile properties of the composites, unlike the results of formal studies.[6] The tensile strength and modulus of modified hemp reinforced composites increased more obviously with the modified hemp content than those of unmodified hemp reinforced composites increased

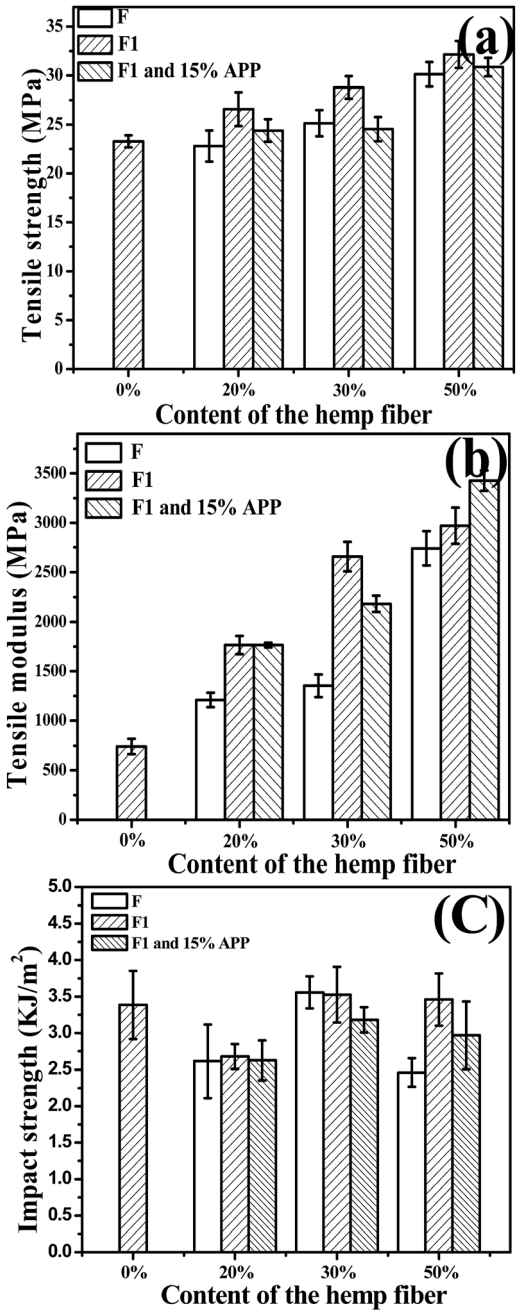

Fig. 5 Effect of hemp fiber loading ratio on the tensile strength (a), tensile modulus (b) of hemp fiber/PP composites and (c) impact strength.

with the unmodified hemp content. The hemp has the better stiffness than PP. On the other hand, the $-O^{-}Ca^{2+}-OH$ produced on the fiber surface may also react with MAPP by the esterification between the anhydride groups of MAPP and the hydroxyl of the $-OCa^{2+}-OH$ on the natural fiber. The interfacial interaction and mechanical properties thus could be much improved.

However, the tensile strength of the composite compounded with treated hemp fiber and 15% APP was always lower than that of composites without APP, although they were still higher

Open Access Article. Published on 23 June 2017. Downloaded on 10/24/2025 10:46:36 PM.
This article is licensed under a Creative Commons Attribution-NonCommercial 3.0 Unported Licence.

than that of the pure PP. This result was caused by the APP insertion, which was supposed to be hydrophilic and likely to upset the interfacial adhesion between the fiber and matrix and thus the mechanical properties. Nevertheless, the modulus of the composites was not affected by the APP insertion as shown in Fig. 5(b). Instead, it increased with the APP insertion maybe because of the rigidity of APP.

Fig. 5(c) shows the impact strength of virgin PP and the composites. The composites with 30% of hemp presented a better impact strength compared with that of the other two contents, and it was also comparable with that of PP. Modification on the hemp did not seem to influence the impact strength of the composites obviously. However, APP insertion in the composites resulted in a worse impact strength of the composites, which revealed the poor interface compatibility between APP and PP.

Morphology observation. Fig. 6 shows the SEM photographs of fractured surfaces of the composite with 50% hemp fiber and different formulation. Fig. 6(a) of untreated hemp fiber/PP composite PPF-50 shows that the interface was worse than that of PPF1-50 with the holes left by the pulled-out fibers. Fibers were pulled out from the matrix during the fracture process, indicating poor interfacial interaction between hemp fiber and PP matrix which resulted in poor composite mechanical properties.[36] Fig. 6(b) of PPF1-50 showed the better interfacial adhesion between modified hemp and PP. Fibers were even split by the fracture before they were pulled out from the matrix, which proved the stronger composite interface. This led to a composite material with excellent mechanical properties. However, the composite interface was the worst with APP insertion (PPF1-50-15R), as shown in Fig. 6(c), in the light that the cracks between the fiber and matrix and the APP powder could be obviously observed. APP aggregation also existed in the matrix and the interface. These resulted in the bad mechanical properties of the composites.

Crystallization behaviour. Table 3 shows the crystallization temperature (T_c), melting temperature (T_m), melting enthalpy (ΔH_m), and the degree of crystallinity (X_c) of the composites obtained from the differential scanning calorimetry (DSC) analysis.

The DSC results showed that the crystallization temperature T_c of all the composites was lower than that of PP (122 °C). The hemp insertion promoted the nucleation and crystallization of PP, and thus lowered the T_c of PP to approximately 112 °C. T_c did not vary with the hemp content apparently. However, T_c of the PPF1 series composites was higher than that of PPF series composites. The modified hemp presented less nucleation effect on PP. The APP insertion did not further decrease the T_c of the untreated hemp fiber-reinforced composites.

The crystallization of composites is controlled by two factors. The reinforcements presented a nucleating effect that caused the crystallization temperature and degree of crystallization to increase. However, the reinforcement restricted the migration and diffusion of polymer chains to the growing polymer crystal in the composites. Thus, the crystallization temperature decreased with the reinforcements because of its negative effect on crystallization.[37,38] In our study, the T_c of all the composites

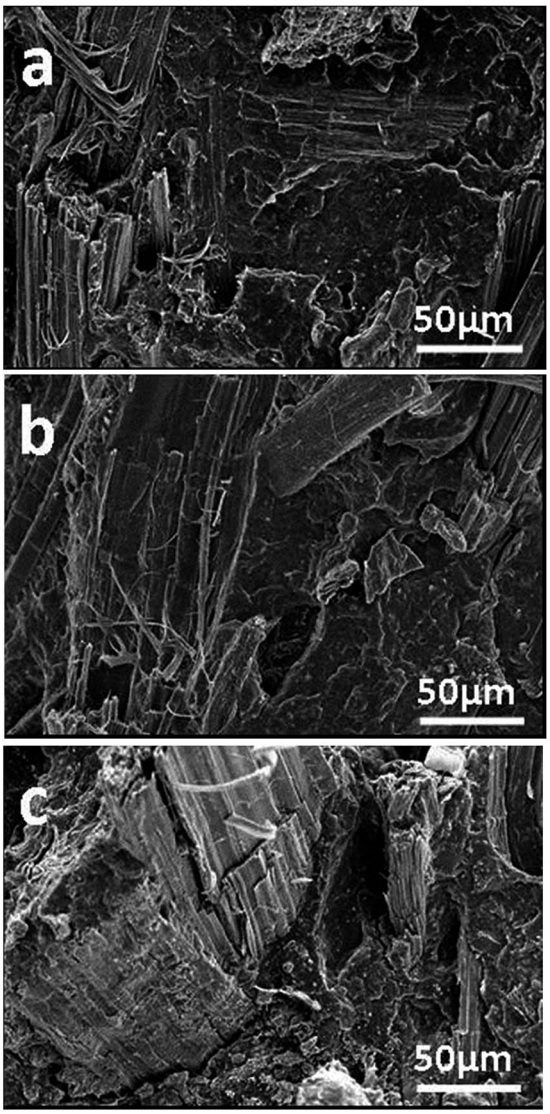

Fig. 6 SEM photos of the fractured composite surface: (a) PPF-50, (b) PPF1-50, (c) PPF1-50-15R composite.

decreased, which should be related to the addition of the hemp and APP. The hemp fibers and APP hindered the migration and diffusion of PP chains to the crystal nucleus in the composites.

The melting temperature (T_m) of the composites was not much different from that of PP and did not change obviously with the composite formulation, as shown in Table 3. This showed that the feature of the crystal formed during the crystallization was not significantly influenced by the hemp and APP insertion.

The XRD curves of hemp fiber reinforced PP composite and pure PP are shown in Fig. 7. The characterized diffraction peaks of pure PP at $2\theta = 13.7°$, $16.6°$, $18.3°$, $21.5°$ and $25.2°$ was correspond to the monoclinic alpha-phase with planes (110), (040), (130), (041), and (060).[39] The diffraction curves of all the composites also presented the same diffraction peak position with those of PP, which also proved the insertion of hemp and APP did not change the crystallization behavior of PP. However,

Open Access Article. Published on 23 June 2017. Downloaded on 10/24/2025 10:46:36 PM.
This article is licensed under a Creative Commons Attribution-NonCommercial 3.0 Unported Licence.

Table 3 Thermal and crystallization properties of PP and the composites

Samples	T_c (°C)	T_m (°C)	ΔH_m (J g^{-1})	X_c (%)	T_5 (°C)	T_{10} (°C)	T_{50} (°C)
PP	122	151	68.76	33.4	431	445	474
PPF-20	110	147	52.93	32.1	357	390	474
PPF1-20	119	150	47.59	28.8	339	379	486
PPF1-20-15R	111	148	43.43	32.5	305	368	482
PPF-30	112	148	42.81	29.7	327	356	471
PPF1-30	119	150	47.44	32.9	291	340	478
PPF1-30-15R	113	149	40.91	36.2	284	325	483
PPF-50	112	148	32.54	31.8	309	345	469
PPF1-50	118	149	35.25	34.4	265	296	481
PPF1-50-15R	113	148	21.37	30.1	265	295	489

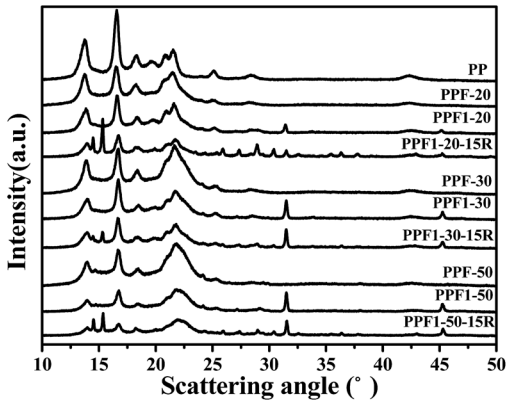

Fig. 7 XRD curves of hemp fiber/PP composite and pure PP.

the intensity of the peaks decreased for the composites with hemp and APP insertion. This means the crystallinity of PP decreased as shown in Table 3, which may be due to the hemp and APP restricting the PP crystallization and the crystal growth.

The diffraction peaks on the curves of PPF1 series at $2\theta = 31.4°$ and $45.2°$ were due to the $Ca(OH)_2$ that was produced and attached on the fiber surface during modification.[40,41] When $Ca(OH)_2$ was exposed in the air, $CaCO_3$ was generated. The diffraction peaks on the curves of PPF1-15R series appeared at $2\theta = 14.5°$ and $15.3°$ was ascribed to be the diffraction peaks of APP.[42] The other small peaks appearing on the curves of APP-inserted composites are brought about by the impurities in the commercial APP.

Thermal stability. Fig. 8(a) shows the thermogravimetric analysis (TGA) thermograms of PP and its composites. The first decomposition occurred in the temperature range of 230 °C to 370 °C indicating the decomposition of hemp fiber and APP, the decomposition of the matrix occurred in the temperature range between 380 °C and 510 °C.[14,15]

Table 3 shows the TGA analysis results, including 5% weight loss temperature (T_5) and 10% weight loss temperature (T_{10}) of PP and composites. All the T_5 of the composites decreased with the increasing fiber content, and the T_5 of the composites were lower than that of the pure PP. This is because of the low thermal stability of the hemicelluloses in hemp.[16] The T_5 value of PPF series of composites were the highest, the PPF1-R series of composites were the lowest. This may be caused by the Ca^{2+}

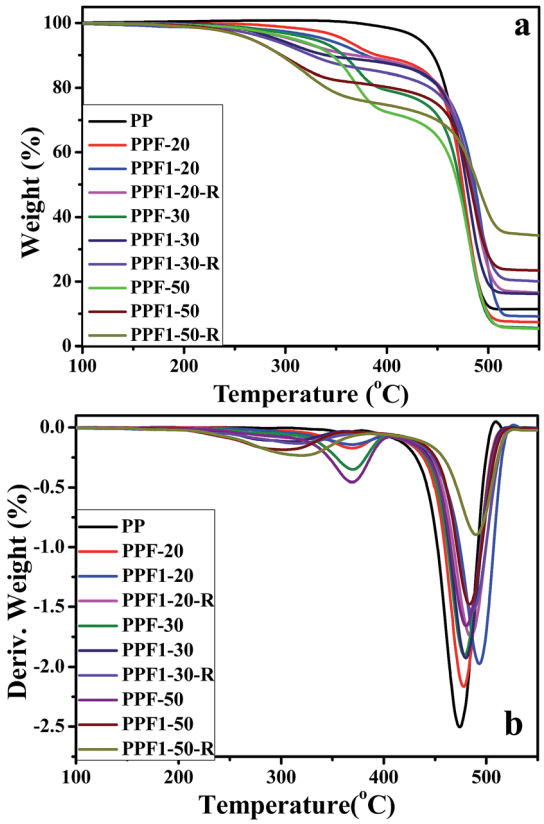

Fig. 8 (a) TGA thermograms of pure PP and the composites; (b) DTG curves of pure PP and the composites.

on the surface of the F1 which could promote the thermal degradation of the hemp fiber to produce $CaCO_3$. The thermal stability of PPF1-R series composites were poor, this may be because the APP releases acid and non-flammable gases when exposed to high temperature; these acids contribute to hemp fiber dehydration and charring.[15] Furthermore, all the T_5 of composites were still higher than 250 °C. This thermal stability of the hemp-reinforced PP composites was good enough for their application in many fields, such as packaging, construction and automotive interiors.

Fig. 8(b) shows the derivative thermogravimetric analysis (DTG) curves of pure PP and composites. Two peaks with maxima ranging between 300 °C to 370 °C and 470 °C to 490 °C

Open Access Article. Published on 23 June 2017. Downloaded on 10/24/2025 10:46:36 PM. This article is licensed under a Creative Commons Attribution-NonCommercial 3.0 Unported Licence.

were observed for the composites. The temperature with the maximum degradation speed (T_{max}) of PP and composites is shown in Table 3. T_{max} increased slightly with the hemp and APP content, which should be related to the high thermal stability of inorganic chemicals.

Conclusions

In this study, the flammability of hemp fiber was improved by the *in situ* treatment of the mixture of NaOH and $CaCl_2$. Calcium alkoxide was produced on the surface of fiber with the treatment, and calcium hydroxide and the calcium carbonate were thereafter absorbed on the fiber surface, which should be helpful in the improvement of the fire retardancy. Thereafter, the flammability of the composites was also improved, and was further improved by APP insertion. The LOI of the PPF1-50 was 23.5, which was much higher than that of PP of 18.5%. When the APP was added, the flammability of the composite was improved by synergistic interaction between freshly produced calcium hydroxide and APP. The LOI of the PPF1-50-15R was increased to 25.5. Furthermore, the comprehensive mechanical properties of composite materials were also much improved according to the mechanical property characterization. The tensile strength of the PPF1-50 composite was increased by 38% compared with that of pure PP. The thermal stability of the hemp fiber/PP composites demonstrated by T_5 was higher than 250 °C, and could be applied in many fields, such as packaging, construction and automotive interiors. XRD characterization proved that calcium salt was produced with the treatment. The XRD and DSC results proved the treated hemp did not apparently change the crystal feature of PP. In other words, the inorganic flame retardant-treated hemp can be applied as a reinforcement for flame retardant biocomposites with excellent properties.

Acknowledgements

The authors would like to thank to the financial support for this project from the National Natural Science Foundation of China (No. 21404013), the Science and Technology Development Plan of Jilin Province, China (No. 20140204039GX and No. 20160101323JC), Changchun Science and Technology Plan Project, China (No. 14KG105), Open Research Fund of State Key Laboratory of Polymer Physics and Chemistry, Changchun Institute of Applied Chemistry, Chinese Academy of Sciences, and the Research Project of Science and Technology of the Education Department of Jilin Province during the 12th Five-year Plan Period (No. 2015-78).

References

1 S. Duquesne, F. Samyn, P. Ouagne and S. Bourbigot, *J. Ind. Text.*, 2015, **44**(5), 665–681.
2 J. T. Kim and A. N. Netravali, *Agric. Food Chem.*, 2010, **58**, 5400–5407.
3 S. A. Paul, K. Joseph, G. Mathew, L. A. Pothen and S. Thomas, *Polym. Compos.*, 2010, **31**, 816–824.
4 T. J. Madera-Santana, H. S. Valdez and M. O. W. Richardson, *Polym. Eng. Sci.*, 2013, **53**, 59–68.
5 L. B. Manfredi, E. S. Rodriguez, M. Wladyka-Przybylak and A. Vazquez, *Polym. Degrad. Stab.*, 2006, **91**, 255–261.
6 N. Suppakarn and K. Jarukumjorn, *Composites, Part B*, 2009, **40**, 613–618.
7 S. L. Du, X. B. Lin, R. K. Jian, C. Deng and Y. Z. Wang, *Chin. J. Polym. Sci.*, 2015, **33**(1), 84–94.
8 M. W. Chai, S. Bickerton, D. Bhattacharyya and R. Das, *Composites, Part B*, 2012, **43**, 2867–2874.
9 A. Rachini, G. Mougin, S. Delalande, J. Y. Charmeau, C. Barres and E. Fleury, *Polym. Degrad. Stab.*, 2013, **97**, 1988–1995.
10 R. Kozlowski and M. Wladyka-Przybylak, *Polym. Adv. Technol.*, 2008, **19**, 446–453.
11 F. Shukor, A. Hassan, S. M. Islam, M. Mokhtar and M. Hasan, *Mater. Des.*, 2014, **54**, 425–429.
12 R. Jeencham, N. Suppakam and K. Jarukumjor, *Composites, Part B*, 2014, **56**, 249–253.
13 A. Subasinghe and D. Bhattacharyya, *Composites, Part A*, 2014, **65**, 91–99.
14 Y. H. Guan, W. Liao, Z. Z. Xu, M. J. Chen and J. Q. Huang, *RSC Adv.*, 2015, **5**, 59865–59873.
15 J. Z. Liang and Y. J. Zhang, *Polym. Int.*, 2010, **59**, 539–542.
16 M. Sain, S. H. Park, F. Suhara and S. Law, *Polym. Degrad. Stab.*, 2004, **83**, 363–367.
17 A. A. Bakar and N. Baharulrazi, *Polym.-Plast. Technol. Eng.*, 2008, **47**, 1072–1079.
18 X. Li, L. G. Tabil and S. Panigrahi, *J. Polym. Environ.*, 2007, **15**, 25–33.
19 A. K. Mohanty, M. Misra and L. T. Drzal, *Compos. Interfaces*, 2001, **8**(5), 313–343.
20 A. E. Sabbagh, *Composites, Part B*, 2014, **57**, 126–135.
21 Marwan and E. Indarti, *Energy Convers. Manage.*, 2016, **117**, 319–325.
22 M. C. Yew, N. H. Ramli Sulong, M. K. Yew, M. A. Amalina and M. R. Johan, *Prog. Org. Coat.*, 2015, **78**, 59–66.
23 R. N. Rothon and P. R. Hornsby, *Polym. Degrad. Stab.*, 1996, **54**, 383–385.
24 M. R. Islam, M. Rivai, A. Gupta and M. D. H. Beg, *J. Polym. Eng.*, 2015, **35**(2), 135–143.
25 H. Sosiati and Harsojo, *Cellul. Chem. Technol.*, 2014, **48**, 33–43.
26 K. O. Reddy, C. U. Maheswari, M. Shukla, J. I. Song and A. V. Rajulu, *Composites, Part B*, 2013, **44**, 433–438.
27 D. Ray, B. K. Sarkar, A. K. Rana and N. R. Bose, *Composites, Part A*, 2001, **32**, 119–127.
28 M. Chabannes, E. Garcia-Diaz, L. Clerc and J. C. Bénézet, *Constr. Build. Mater.*, 2016, **102**, 821–833.
29 L. X. Bao, S. M. Yang, X. Luo, J. X. Lei, Q. Cao and J. L. Wang, *Appl. Surf. Sci.*, 2015, **357**, 564–572.
30 A. E. F. S. Almeida, G. H. D. Tonoli, S. F. Santos and H. Savastano Jr, *Cem. Concr. Compos.*, 2013, **42**, 49–58.
31 V. D. Pizzol, L. M. Mendes, L. Frezzatti, H. Savastano Jr and G. H. D. Tonoli, *Miner. Eng.*, 2014, **59**, 101–106.
32 G. H. D. Tonoli, V. D. Pizzol, G. Urrea, S. F. Santos, L. M. Mendes, V. Santos, V. M. John, M. Frías and H. Savastano Jr, *J. Mater. Sci.*, 2016, **51**, 7929–7943.

 This journal is © The Royal Society of Chemistry 2017

Open Access Article. Published on 23 June 2017. Downloaded on 10/24/2025 10:46:36 PM.
This article is licensed under a Creative Commons Attribution-NonCommercial 3.0 Unported Licence.

33 S. S. L. Sobhana, D. R. Bogati, M. Reza, J. Gustafsson and P. Fardim, *Microporous Mesoporous Mater.*, 2016, **225**, 66–73.
34 C. Quan, N. B. Gao and Q. B. Song, *J. Anal. Appl. Pyrolysis*, 2016, **121**, 84–92.
35 F. Samyn, S. Bourbigot, S. Duquesne and R. Delobel, *Thermochim. Acta*, 2007, **456**, 134–144.
36 P. Sudhakara, A. P. K. Devi, C. V. Prasad, K. O. Reddy, L. D. Woo, B. S. Kim and J. I. Song, *J. Appl. Polym. Sci.*, 2013, **128**, 976–982.
37 M. S. Huda, L. T. Drzal, M. Misra, A. K. Mohanty, K. Williams and D. F. Mielewski, *Ind. Eng. Chem. Res.*, 2005, **44**, 5593–5601.
38 C. Albano, J. Papa, M. Ichazo, J. Gonzalez and C. Ustariz, *Compos Struct.*, 2003, **62**, 291–302.
39 F. Adam and M. S. Wong, *Catal. Commun.*, 2011, **13**, 87–90.
40 M. I. Zaki, H. Knozinger, B. Tesche and G. A. H. Mekhemer, *J. Colloid Interface Sci.*, 2006, **303**, 9–17.
41 H. J. Lin, H. Yan, B. Liu, L. Q. Wei and B. S. Xu, *Polym. Degrad. Stab.*, 2011, **96**, 1382–1388.